# Resting-state functional connectivity analysis of the mouse brain using intrinsic optical signal imaging of cerebral blood volume dynamics



doi: 10.1088/1361-6579/aac033

# Resting-state functional connectivity analysis of the mouse brain using intrinsic optical signal imaging of cerebral blood volume dynamics

To cite this article before publication: Yuto Yoshida *et al* 2018 *Physiol. Meas.* in press https://doi.org/10.1088/1361-6579/aac033

**Title: Resting-state functional connectivity analysis of the mouse brain using intrinsic optical signal imaging of cerebral blood volume dynamics**

**Authors:** Yuto Yoshida[1, 2], Mitsuyuki Nakao[2], Norihiro Katayama[2*]

* Corresponding author, e-mail: katayama@ecei.tohoku.ac.jp

**Address:** 6-6-05, Aza-Aoba, Aramaki, Aoba-ku, Sendai, Miyagi prefecture, 980-8579, Japan

1. Research Fellow of Japan Society for the Promotion of Science (JSPS)

2. Biomodeling Laboratory, Graduate School of Information Sciences, Tohoku University, Japan

**Abstract:**

*Objective:* Resting-state functional connectivity (rsFC) of the human brain is closely related with neurological and psychiatric disorders. Mice are widely used to investigate the physiological mechanisms of such disorders, because of the applicability of invasive experimental techniques. Thus, studies on rsFC of the mouse brain are essential to link physiological mechanisms with these disorders in humans. In this study, we investigated the applicability of intrinsic optical signal imaging of cerebral blood volume (IOSI-CBV) for rsFC analysis of the mouse brain.

*Approach:* Transcranial IOSI-CBV images were collected from the brains of un-anesthetized wild-type mice with a cooled-CCD camera. The time traces of all pixels were averaged to create a global signal (GS). Marginal and partial correlation analyses were performed to estimate the rsFC based on CBV signals both with and without GS removal. The consistency of the results were confirmed by comparing them with to the rsFCs data reported in the previous studies.

*Main results:* We confirmed that GS correlated with heart rate fluctuation in the FC frequency band. The marginal correlation coefficient of CBV with GS removal was consistent with measurements using conventional optical imaging methods relying on oxygenated hemoglobin concentration and cerebral blood flow.

*Significance:* These results suggest the applicability and usefulness of the transcranial IOSI-CBV method to estimate rsFC of the mouse brain.

Keyword: resting-state functional connectivity, intrinsic optical signal imaging, cerebral blood volume, mouse model of human rsFC, global signal, hemodynamics

## 1. Introduction

Signals of spontaneous brain activity contains valuable information regarding brain health. Many studies using functional magnetic resonance imaging (fMRI) of the human brain have reported distinctive spatiotemporal dynamics observed during the resting-state (van den Heuvel and Hilleke E 2010). In particular, functional connectivity (FC), which characterizes temporal synchronicity among multiple brain regions, has attracted attention (van den Heuvel and Hilleke E 2010). Interestingly, patterns of resting-state FC (rsFC) are closely related to neurological and psychiatric disorders including cerebral infarction (Carter *et al* 2010), schizophrenia (Zhou *et al* 2007, Lynall et al 2010), autism spectral disorder (Gotts *et al* 2012), bipolar disorder (Öngür *et al* 2010), and depression (Sheline *et al* 2010, Greicius *et al* 2007). Thus, rsFC analysis is expected to emerge as a next-generation diagnostic method for cerebral disorders.

To study mechanisms of cerebral disorders, mice are widely used because of the ability to conduct invasive experimental techniques, such as microelectrode implantation for local field potential recording (Sigurdsson *et al* 2010), and optogenetic stimulation (Ishizuka *et al* 2006). These invasive techniques are essential for investigating potential causal relationships between rsFC and these various brain disorders. Thus, translational studies are an important link between findings in mice and in humans. However, due to the small size of the mouse brain, application of fMRI to the mouse is difficult and there are many severe constraints limiting this experimental condition (Sforazzini *et al* 2014).

In many rsFC studies of the mouse brain, optical imaging of hemodynamic signals has been adopted instead of fMRI because it is significantly easier to perform. There are various reports describing the use of intrinsic optical signal imaging (IOSI) to measure change in oxygenated hemoglobin concentration (IOSI-HbO) (White *et al* 2011, Bauer *et al* 2014, Bergonzi *et al* 2015, Guevara *et al* 2013, Bero *et al* 2012). Cerebral blood flow (CBF) measured by laser speckle contrast imaging (LSCI) has also been used (Bergonzi *et al* 2015, Guevara *et al* 2013). To monitor spatiotemporal neural activity of the brain, cerebral blood volume (CBV) imaging (IOSI-CBV) is also available, as a lower cost IOSI technique. It has been reported that these IOSI signals are coupled with neuronal activity (Sheth *et al* 2004). Among the IOSI signals, CBV is directly responsive to the neurovascular coupling mechanism, suggesting closer expression of neural activity (Sforazzini *et al* 2014, Mateo *et al* 2017). However, no reports have described the use of the IOSI-CBV method to analyze rsFC of the mouse brain.

Many FC studies have used Pearson's correlation coefficient (marginal correlation) to measure the strength of interaction between brain regions. However, marginal correlation does not imply actual connectivity between the regions. To extract "direct" or "effective" connectivity in the brain, partial

correlation analysis has proved to be useful in human fMRI studies (Marrelec *et al* 2006, Fransson and Marrelec 2008). However, it has not been applied to optically monitor hemodynamic signals of the mouse brain.

In this study, we apply IOSI-CBV to measure spontaneous activity of the mouse brain, in an un-anesthetized, awake, and head restrained condition, to analyze rsFC. Marginal and partial correlation analyses are performed to estimate architecture of the resting-state mouse brain. In addition, consistency of the results is evaluated by comparing them to rsFC data reported in previous studies.

## 2. Materials & Methods

### 2.1 Animal Preparation

All experimental procedures were approved by the Institutional Animal Care and Use Committee of Tohoku University and were performed according to the Japanese Government Animal Protection and Management Law (No. 105). All efforts were made to minimize animal suffering. Six male mice (C57BL/6, 23-25 g) were used for this study. The data for one mouse was omitted because of insufficient signal-to-noise ratio. Surgical operations were performed with isoflurane anesthesia (1-2%) and local application of xylocaine. The skull was exposed by removing the scalp. Stainless steel screws for recording neocortical electroencephalograms (EEGs) were fixed to the skull outside the field of view and an O-shaped plastic plate was fixed onto the skull with dental acrylic cement. Twisted stainless steel wires were implanted in the neck of the animal to monitor EMGs and ECG signals.

### 2.2 Recording

Following recovery from the surgery (approximately 1 week), experiments were performed over four consecutive days, in order for the mice to become adapted to the environment. Each mouse was transferred to the stage of an upright microscope (BX50WI, Olympus, Japan) in a dark shielded cage. The head of the mouse was fixed by clamping the plastic plate with a custom-made holder. The skull was moisturized with saline and covered with liquid paraffin to prevent drying and to keep the skull transparent (Tohmi *et al* 2009). To obtain CBV signals from the cortex, green light illumination at an isosbestic wavelength of oxygenated/deoxygenated hemoglobin (~525 nm) was provided by a Xenon lamp (LA-410UV3, Hayashi-watch works, Japan) or a low-noise LED (Mic-LED-530, Prizmatix, Israel) through a bandpass filter (523±5 nm, Andover, USA) (Sheth *et al* 2004, Ma *et al* 2016, Haglund and Hochman 2007). Images of green light reflected from the cortex were acquired transcranially with a cooled CCD camera (C9100-13, Hamamatsu Photonics, Japan) at 28 fps (128 × 128 pixels, field of view: 6 mm × 6 mm). Simultaneously, electrophysiological signals (EEGs, EMGs, and ECGs) were amplified and sampled at 1 kHz along with the CCD exposure timing signal.

## 2.3 Preprocessing

The acquired images were binned (binning size: $4 \times 4$, final resolution: $32 \times 32$) to increase signal-to-noise ratio and to reduce data size. The light source noise caused by the Xenon lamp fluctuation was reduced by the ICA-based noise reduction algorithm (Yoshida *et al* 2015a, Yoshida *et al* 2015b). The wakefulness of the animal was determined on the basis of the EEG and EMG signals (Veasey *et al* 2000). Only data collected during quiet wakefulness were used in this study.

## 2.4 Image processing

Assume that the intensity of reflection light $I$ and absorption coefficient of the brain tissue $\mu$ obey the Modified Beer-Lambert Law (MBLL) (Kocsis *et al* 2006, Delpy *et al* 1988):

$$-\ln(I/I_0) = L\mu + G, \tag{1}$$

where ln() is the natural logarithm, $L$ is the path length of detected photons and $G$ is a geometry-dependent factor, which is independent of absorption. In addition, we also assume the following relationships:

$$-\ln(I_b/I_0) = L\mu_b + G, \tag{2}$$

$$\Delta I = I - I_b, \tag{3}$$

$$\Delta\mu = \mu - \mu_b, \tag{4}$$

where $I_b$ and $\mu_b$ are baseline components of the respective variables. Arranging eqs. (1)-(4), we obtain:

$$-\ln(I/I_b) = L\Delta\mu \tag{5}$$

$$-(\Delta I/I_b) = 1 - e^{-L\Delta\mu}. \tag{6}$$

For $\left|1 - e^{-L\Delta\mu}\right| \ll 1$, the following approximation holds:

$$1 - e^{-L\Delta\mu} \approx L\Delta\mu. \tag{7}$$

On the other hand, $\mu$ is related to the cerebral blood volume in the tissue $C_{CBV}$ as follows (Kocsis *et al* 2006):

$$\Delta\mu \propto \Delta C_{CBV}, \tag{8}$$

Finally, we obtain the following relationship:

$$\Delta C_{CBV} \propto -(\Delta I/I_b). \tag{9}$$

In this study, $I_b$ was estimated by low-pass filtering (<0.0005 Hz) of $I$. According to our experimental data, we have $\left|1 - e^{-L\Delta\mu}\right| = |\Delta I/I_b| < 0.05$. The CBV signal ($x = -(\Delta I/I_b)$) was filtered to the functional connectivity band (FCB, 0.009-0.08 Hz), according to previous studies (Bauer *et al* 2014, White *et al* 2011). The time traces of all pixels were averaged to create a global signal (GS). The GS removal was performed by regression in the CBV signal of each site (White *et al* 2011).

## 2.5 Analysis

*Instantaneous heart rate fluctuation.* Instantaneous heart rate (IHR) was estimated from the time series of the reciprocal of the intervals between the event time of the R wave in ECGs spaced by the interval event time (Deboer *et al* 1984, Mitsuyuki *et al* 1997). In order to detect R waves, a high-pass filter (>51 Hz) and matched filter (Bancroft 2002) with a clear R wave as template were applied to the ECG. Time periods contaminated by a strong EMG noise were masked and IHR were linearly interpolated in the masked period. Then the IHR was linearly interpolated and resampled simultaneously with CBV data for cross correlation analysis.

*Functional connectivity analysis.* In order to estimate the functional connectivity between the cortical regions, 14 seeds were positioned at the following cortical regions of both hemispheres: primary motor (M1, [anterior +0.86 mm, lateral ±1.84 mm]), secondary motor (M2, [+1.42, ±0.75]), primary somatosensory (S1, [–0.46, ±2.10]), parietal association (PtA, [–1.70, ±1.40]), retrosplenial dysgranular (RSD, [–2.18, ±0.50]), primary visual (V1, [–3.52, ±2.25]) and secondary visual (V2, [–2.70, ±1.49]), according to a histological atlas (Franklin and Paxinos 2008). The seed positions were scaled to adjust to the size of the brain based on the distance between bregma and lambda of the skull (4.1 mm for reference). A few seed positions were appropriately shifted slightly to avoid thick blood vessels.

For marginal correlation analysis, Pearson's correlation coefficient $R_{i,j}$ was calculated for each pair of CBV data $x(i,t)$ and $x(j,t)$, where $i$ and $j$ represent the position index number. The marginal correlation matrix was given by $\mathbf{R} = (R_{i,j})$. The partial correlation matrix $\mathbf{\Pi} = (\Pi_{i,j})$ was calculated according to the following definition (Guttman 1940):

$$\Pi_{i,j} = (-1)^{i+j} \frac{C_{i,j}}{\sqrt{C_{i,i} C_{j,j}}}, \tag{10}$$

where $C_{i,j}$ represents the $(i,j)$-th cofactor of the marginal correlation matrix $\mathbf{R}$.

*Extraction of numerical values from color-coded correlation maps.* To evaluate the consistency of the results of the present studies with the previous conventional ones, the magnitude of each functional connectivity (correlation coefficient) was compared (see discussion). Unfortunately, in the previous studies, correlation coefficients were not provided as numerical values but images of color-coded correlation maps. Hence, we developed a simple MATLAB script to extract numerical values from the images. Briefly, images of color-coded correlation maps with color bars were imported from PDF files into the MATLAB workspace. The script decoded the numerical value of the coefficient by minimizing the distance in the Red-Green-Blue color space between the color of the pixel representing the coefficient and that of the color bar.

Figure 1

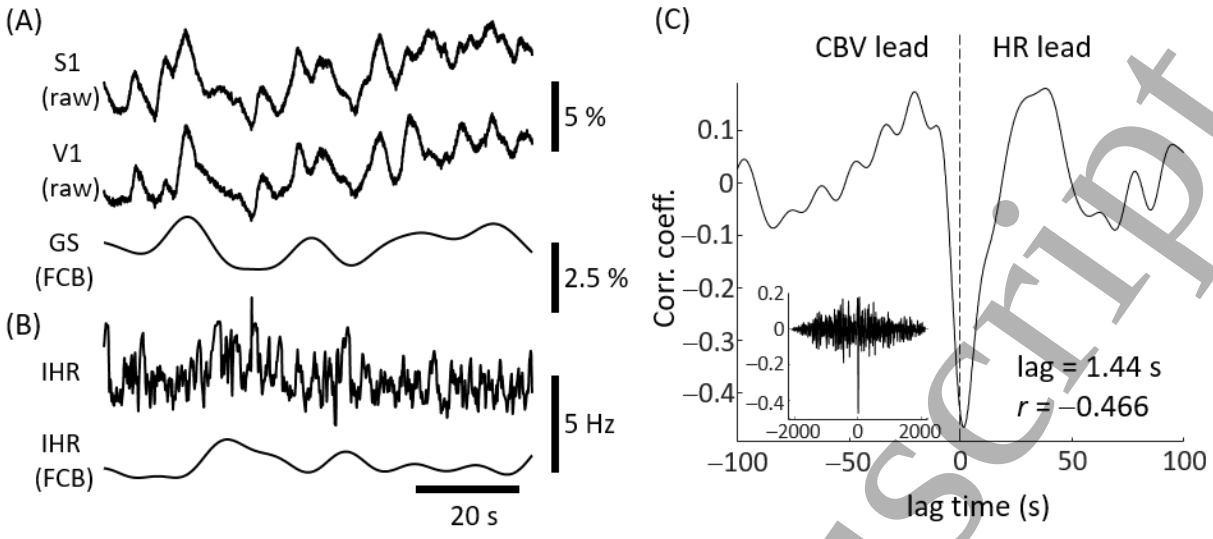


Figure 1: Correlated dynamics of cerebral blood volume (CBV) changes and heart rate fluctuations. (A) Time courses of IOSI-CBV signals and the global signal in the functional connectivity band (FCB, 0.009-0.08 Hz). (B) Time courses of the instantaneous heart rate (IHR), and its FCB component simultaneously recorded with the IOSI-CBV. (C) Cross-correlation function between the global signal (FCB) and the IHR (FCB).

# 3. Results

## 3.1 Spatiotemporal profiles of IOSI-CBV signals

Similar to conventional fMRI (Chai *et al* 2012, Sforazzini *et al* 2014) and IOSI-HbO studies (Guevara *et al* 2013), raw CBV signals were almost spatially synchronized (Fig. 1A). In previous studies, the hemodynamic signal was often assumed to be composed of a spatially uniform global signal and residuals expressing local neural activity. It has been reported that the global signal correlates with heart rate fluctuation (Chang *et al* 2013, Shmueli *et al* 2007). Hence, we calculated cross-correlation functions between the global signal and the instantaneous heart rate (IHR) in the functional connectivity band (FCB, 0.009-0.08 Hz) (Fig. 1A-C). We confirmed that these signals were negatively correlated and the change in IHR preceded the GS. In this case, the lag time was 1.4 s ahead of the CBV. The heart rate regressor explained approximately 20% of the variance of the global signal. It has been reported that the heart rate fluctuation partially reflects autonomic nervous system activity (Pomeranz *et al* 1985) that is independent from the local neural activity of the brain. Hence, the global signal has been removed from the hemodynamic signal before correlation analysis in many rsFC studies (White *et al* 2011, Guevara *et al* 2013). In this study, we also performed this preprocessing (GS removal) for some of the correlation analysis.

Figure 2B shows the spatio-temporal structure of the CBV signals when the global signal (GS) was removed by regression in the CBV signal of each site. Naturally, spatial synchronicity was reduced, however some brain regions, such as M1 and S1, still expressed synchronized activity. We calculated marginal correlation coefficients of the CBV signals in a seed and all of the other sites, to generate a correlation map. As shown in Fig. 2C, the overall correlation maps were bilaterally symmetric. Highly correlated areas were observed around the seeds with unique shapes. These maps were similar to those reported in previous studies using IOSI-HbO (White *et al* 2011) and LSCI-CBF (Bergonzi *et al* 2015) methods, also with GS removal during preprocessing.

Figure 2

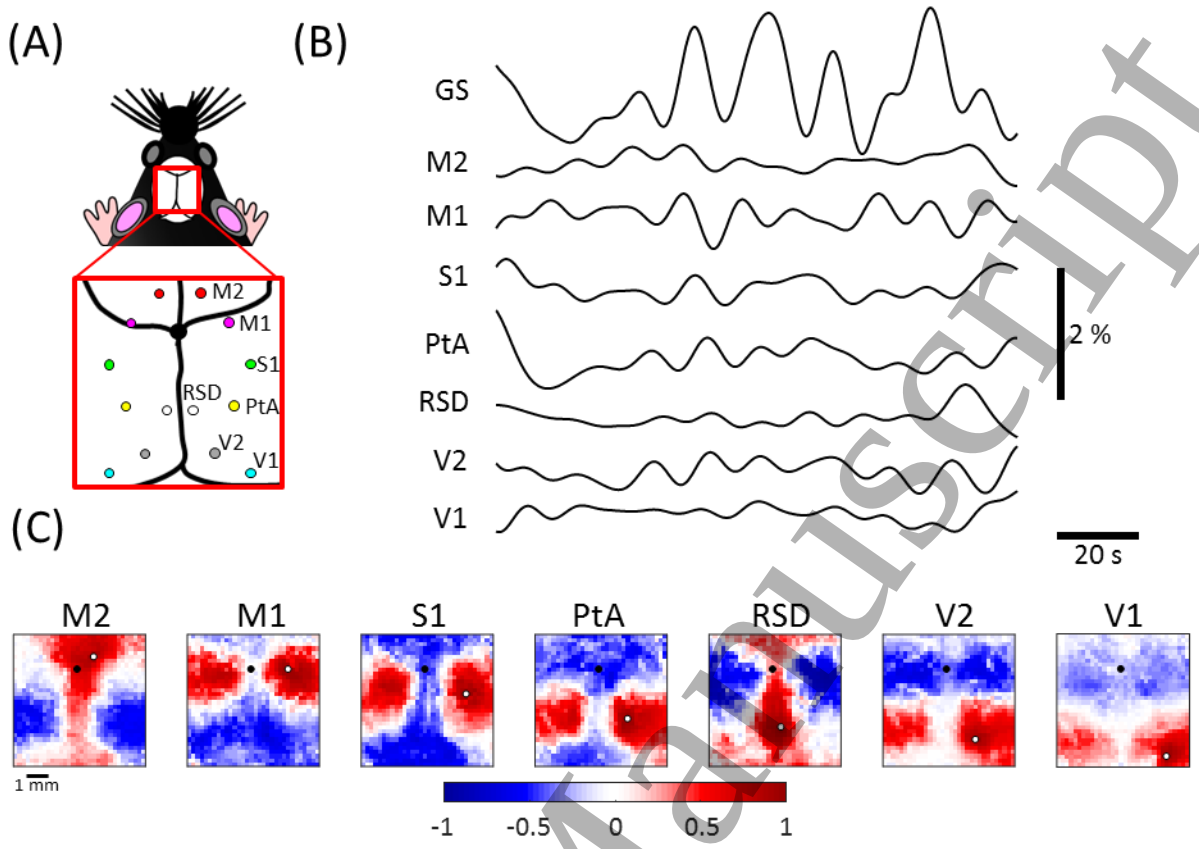


Figure 2: Functional mapping of the mouse neocortex by IOSI-CBV. (A) The field of view of the optical imaging and seed positions. (B) Time course of the global signal and local signals observed in the respective cortical areas (right hemisphere). (C) Seed-based correlation maps. Positions of ascertaining seeds and of bregma are shown with white and black circles, respectively. See text for abbreviations.

### 3.2 Marginal correlation analysis of the IOSI-CBV signals

In order to estimate rsFC of the mouse cortex using the CBV signals, marginal correlation matrices were calculated from IOSI-CBV data following GS removal. Correlation coefficients were transformed to Fisher's z-scores, averaged across the animal, and inversely transformed to obtain an averaged correlation coefficient (Fig. 3A). Using a thresholding method (threshold = 0.4), coefficients were partially extracted to generate network diagrams (Figs. 3B and C). The threshold value was roughly determined according to Guevara et al (2013) and slightly shifted to separate a distribution of strong positive correlation coefficients from the distribution in which the coefficients were almost zero (zero clusters).

Figure 3A shows the average marginal correlation matrix of resting-state mice (n = 5). Focusing on the positive correlations, all of the functional areas were bilaterally connected with their respective contralateral regions. The observed area could then be roughly divided into 3 groups (subnetworks), according to the positive correlations: (a) bilateral M2, (b) bilateral M1 and S1, and (c) bilateral PtA, RSD, V1 and V2 (Fig. 3B). These subnetworks were negatively correlated with each other (Fig. 3C). Strong negative correlations were found specifically with M2 – S1, M2 – PtA, (M1+S1) – (V2), and RSD – S1 (Fig. 3A-C).

### 3.3 Partial correlation analysis of the IOSI-CBV signals

Next, we calculated partial correlation matrices from IOSI-CBV data following GS removal to examine effective connectivity (Figs. 3D-F). The network diagram was generated similar to marginal correlation analysis (threshold = 0.2). We confirmed that the overall functional connectivity was weaker than the marginal correlation analysis (Fransson and Marrelec 2008, Wang *et al* 2016). Interhemispheric positive correlations were detected in the motor, somatosensory, PtA and RSD cortex. However, interhemispheric correlations within the visual cortex was not evident. In this study, the experiments were performed in a dark cage, thus the visual cortex would not be activated, which could underlie the weak correlations observed. Negative connectivity was weaker than the marginal correlation analysis as well. However, interhemispheric negative connections remained.

To examine the effect of GS removal on the rsFC analysis, we calculated partial correlations of the CBV signals without GS removal (Fig. 3G-I). Focusing on the positive correlation (Fig. 3H), the overall structure was almost the same as in Fig. 3E. The adjacent regions and the contralateral regions were positively linked. As a result, all of the regions were connected to a single network. However, the negative connections were markedly fewer than in the other cases (Fig. 3I). Thus, the partial

correlations of CBV signals without GS removal only provided information of interhemispheric correspondence and spatial closeness between the functional regions.

Figure 3

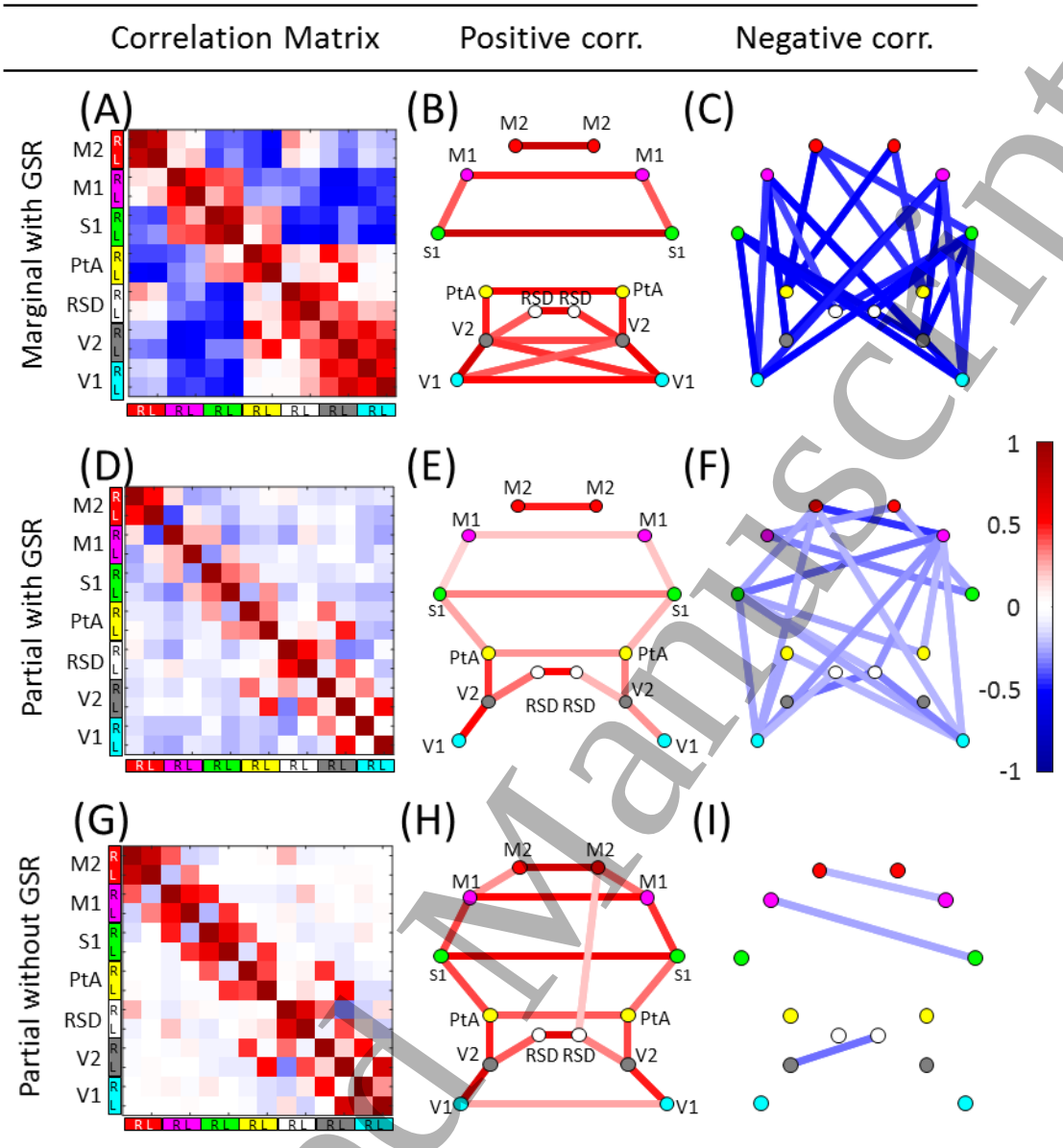


Figure 3: (A, B, C) Marginal correlation analysis for IOSI-CBV with GS removal. (D, E, F) Partial correlation analysis for IOSI-CBV with GS removal and (G, H, I) without GS removal. (A, D, G) Correlation matrixes. Magnitude of the correlation coefficient $(r)$ is color-coded according to the color bar (right hand side). In the correlation network diagrams (B, C, E, F, H, I), neocortical regions are represented as nodes (circles) and correlation coefficients between regions are depicted as color-coded edges. Only the edges with $|r| >$ threshold are drawn, where the threshold value for the marginal and the partial correlations are set to 0.4 and 0.2, respectively.

## 4. Discussion

To assess the plausibility of the rsFC of the mouse brain by using IOSI-CBV, each correlation coefficient was compared with that estimated by IOSI-HbO (White *et al* 2011, Bauer *et al* 2014, Bergonzi *et al* 2015, Guevara *et al* 2013, Bero *et al* 2012) and LSCI-CBF (Bergonzi *et al* 2015, Guevara *et al* 2013). Figure 4 shows a summary of the marginal correlation coefficients estimated by those methods. The estimated correlation coefficient is consistent across the imaging methods and research groups, with the exception of one (Fig. 4g), which was due to low signal-to-noise ratio of the measurement (Guevara *et al* 2013). Therefore, this strongly suggests that IOSI-CBV can provide reliable data for rsFC analysis of the mouse brain.

There are many studies supporting coupling between the optically measured HbO and CBV signals in the brain (Ma *et al* 2016, Mayhew *et al* 2000, Sforazzini *et al* 2014). However, it has been reported that dissociation of changes in HbO and CBV signals is observed by optical imaging with a higher spatial resolution (Haglund and Hochman 2007). Change in the CBV signals in response to an electrical stimulation was reported to be observed in the nerve tissue around the electrode, whereas the change in HbO signal was dominant in the vein. Because of recent advances in brain imaging technology, functional mapping of the human brain is becoming more detailed (Glasser *et al* 2016, Feinberg *et al* 2016). In studies of the mouse brain, spatial resolution of functional mapping are expected to be analyzed at increasingly higher resolution as well (Sforazzini *et al* 2014). Considering the size of the mouse brain compared with a human brain, the CBV signal rather than HbO is likely to be more appropriate for estimating neural activity in the mouse brain.

So far, the IOSI-HbO method has been widely used under the assumption that the HbO signal is close to an fMRI signal and that it would be suitable for comparing the conventional fMRI studies (Pouratian *et al* 2002). The LSCI-CBF method allows functional mapping of the blood perfusion in the brain, which cannot be achieved with the IOSI-CBV method. However, as shown in Fig. 4, the IOSI-CBV method is comparable to all these methods in the rsFC analysis of the mouse brain. In addition, the IOSI-CBV method is cost-effective compared to the IOSI-HbO and LSCI-CBF methods as mentioned above. Therefore, the IOSI-CBV method can be a powerful option for the rsFC analysis of the mouse brain.

To create network diagrams, relatively strong rsFCs were extracted by applying a simple threshold method to the correlation coefficients (Fig. 3). Using marginal correlation analysis, both positive and negative correlation networks were almost symmetrical. These results are consistent with previous research reports using IOSI-HbO (e.g. Bauer *et al* 2014, White *et al* 2011) and fMRI (Sforazzini *et al* 2014). The number of edges in the positive correlation network was almost 20% of the possible edges

in all analysis methods used (Figs. 3B, E and H). However, the number of negative edges showed variability between different analysis methods. The positive correlation networks were easily extracted by the threshold method since the positive correlation coefficients form distinct clusters. In contrast, the absolute values of the negative coefficients were in general small and their variation was large. It was difficult to separate them from zero clusters. This property may have corrupted the symmetry of negative correlation networks calculated by partial correlation analysis (Figs. 3F and I).

In this study, it was shown that the positive correlation network estimated by marginal correlation analysis of the observed area can be roughly divided into three subnetworks (Fig. 3B), whereas partial correlation analysis distinguishes two subnetworks (Fig. 3E). This difference might be explained by characteristics of each correlation analysis. The marginal correlation coefficient reflects the influence of both the coupling between areas and the common driver. Since both are important factors for collaboration, the marginal correlation would be suitable for extraction of *functionally* connected regions. The S1-M1 subnetwork (Fig. 3B) has indeed been identified as the sensorimotor network in rsFC studies (White *et al* 2011, Sforazzini *et al* 2014). The partial correlation analysis is the method to extract node-to-node connections by suppressing the influence of any common driver, thus it is suitable for extracting direct connections. Therefore, the subnetworks in which neighboring regions are connected can be extracted by partial correlation analysis (Fig. 3E) and the number of cortical subnetworks is smaller than those derived from marginal correlation analysis.

Since hemodynamic signals exhibit widely synchronized activity in the brain, a simple correlation analysis does not extract distinct connection patterns. Thus, a spatially homogeneous component called global signal (GS) was estimated and removed from the observed signals before correlation analysis. This preprocessing has been widely used in rsFC analysis. As shown in Fig. 1, GS obtained from IOSI-CBV data also correlated with heart rate fluctuation. It is known that GS also contains noise such as breathing and body movement (Liu *et al* 2017). Thus, the primary objective of GS removal is noise reduction. However, since GS also contains components derived from neural activity, there is criticism that GS removal processing emphasizes negative correlations. In fact, this was seen in our results, as well (Figs. 3F and 3I). The appropriateness of the GS removal processing continues to be actively discussed, and is not yet not resolved (Liu *et al* 2017, Fox *et al* 2009, Murphy *et al* 2009).

To overcome these problems, various analyses including partial correlation analysis (Marrelec *et al* 2006, Fransson and Marrelec 2008) and independence component analysis (Burgess *et al* 2016, Power *et al* 2017) have been conducted. Hence, we performed partial correlation analysis and investigated the effect of GS removal. The impact of GS removal on positive connectivity was relatively modest, however, the impact was very marked on the negative ones (Fig. 3D-I). However, due to limitation of the transcranial IOSI used in this study, available data were restricted in a part of cortex of the brain. Hence, it is impossible to exclude the pseudo correlation caused by the activity in the deep brain

region. Therefore, it should be noted that the partial correlation analysis based on the intrinsic optical signal imaging methods inherently incomplete.

So far, various biological parameters such as blood pressure (Murphy *et al* 2013), respiration, electromyogram, and nerve activity (Liu *et al* 2017) have been reported to correlate with GS as well as heart rate fluctuations. However, it is not clear whether these correlations represent the effects of organs on brain activity. In order to identify physiological networks of complex biological systems, a research field called network physiology is now attracting attention (Bashan *et al* 2012, Bartsch *et al* 2015, Ivanov *et al* 2016, Lin *et al* 2016), which studies the interactions between different organs. By using this framework, it may be possible to investigate the influence of distinct organs on the brain activity.

Figure 4

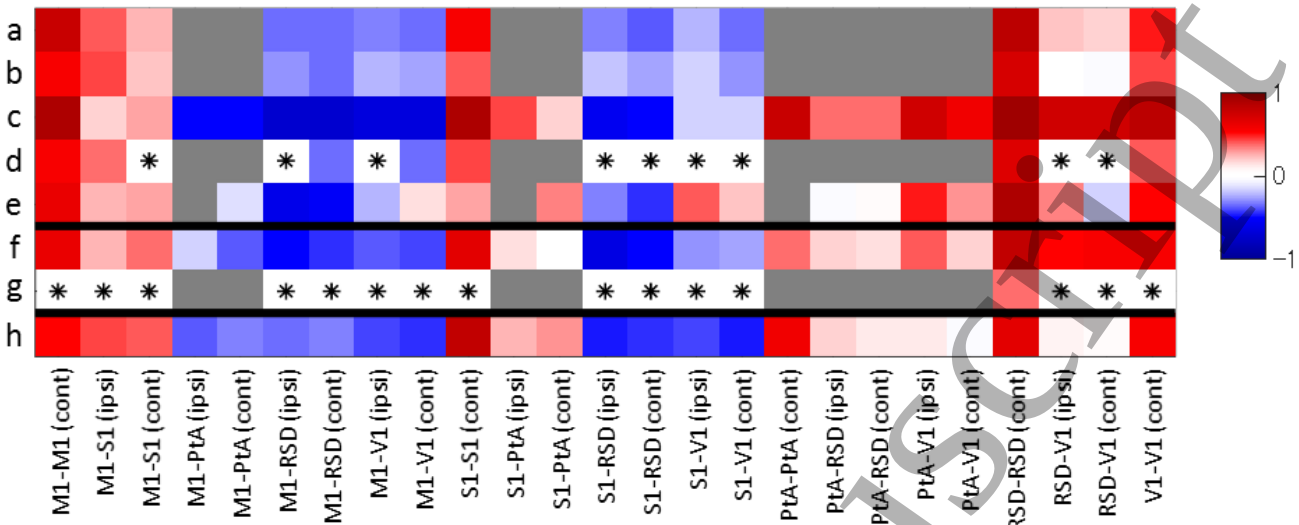


Figure.4: Summary of FC of the mouse brain estimated by using various optical imaging methods. The data for marginal correlation coefficients with GS removal were gathered from the articles and rearranged as a color-coded matrix according to the color bar. (a-e) IOSI-HbO methods, (f and g) LSCI-CBF methods. (h) IOSI-CBV method (the present study). (a) Bauer *et al* 2014, (b) Bero *et al* 2012, (c and f) Bergonzi *et al* 2015, (d and g) Guevara *et al* 2013, (e) White *et al* 2011. Gray cells indicate that the correlation of the pair was not evaluated in the article. White cells with an asterisk indicate that the data was not described in the article because the absolute value of the coefficient was below the threshold determined in the article (= 0.3).

## 5. Conclusions

In this study, we investigated the applicability of cerebral blood volume (CBV) signals transcranially measured by intrinsic optical signal imaging (IOSI) method to analyze resting-state functional connectivity (rsFC) in un-anesthetized wild mice. We confirmed that raw CBV signals were spatially synchronized due to a global signal (GS), which was correlated with heart rate fluctuation in the rsFC frequency band. Marginal and partial correlation analyses were performed to estimate rsFC based on the CBV signals with and without GS removal. It was shown that the marginal correlation coefficients of the CBV signals after GS removal was consistent with that measured by using conventional methods (IOSI-HbO and LSCI-CBF). It was shown that the marginal correlation analysis with GS removal would more clearly depict dissociated groups of functional regions. Partial correlation analysis with GS removal extracted sparser functional connectivity than the marginal one. These results suggest that the combination of IOSI-CBV method and marginal correlation analysis with GS removal is useful to characterize the rsFC network in mouse brain.

## Acknowledgements

*This research was supported in part by the MEXT/JSPS KAKENHI Grant Numbers JPK15K012760 (NK), JP16S420010 (NK), JP16H06276 (NK), and JP17J02254 (YY).*

## References


Bancroft J C 2002 Introduction to matched filters *CREWES Res. Rep.* **14** 1–8

Bartsch R P, Liu K K L, Bashan A and Ivanov P C 2015 Network physiology: How organ systems dynamically interact *PLoS One* **10** 1–36

Bashan A, Bartsch R P, Kantelhardt J W, Havlin S and Ivanov P C 2012 Network physiology reveals relations between network topology and physiological function *Nat. Commun.* **3** 702 Online: http://dx.doi.org/10.1038/ncomms1705

Bauer A Q, Kraft A W, Wright P W, Snyder A Z, Lee J M and Culver J P 2014 Optical imaging of disrupted functional connectivity following ischemic stroke in mice *Neuroimage* **99** 388–401

Bergonzi K M, Bauer A Q, Wright P W and Culver J P 2015 Mapping functional connectivity using cerebral blood flow in the mouse brain *J. Cereb. Blood Flow Metab.* **35** 367–70 Online: http://www.nature.com/doifinder/10.1038/jcbfm.2014.211

Bero A W, Bauer A Q, Steward F R, White B R, Cirrito J R, Raichle M E, Culver J P and Holtzman D M 2012 Bidirectional Relationship between Functional Connectivity and Amyloid-β Deposition in Mouse Brain *J. Neurosci.* **32** 4334–40 Online: http://www.jneurosci.org/content/32/13/4334.full.pdf

Burgess G C, Kandala S, Nolan D, Laumann T O, Power J D, Adeyemo B, Harms M P, Petersen S E and Barch D M 2016 Evaluation of Denoising Strategies to Address Motion-Correlated Artifacts in Resting-State Functional Magnetic Resonance Imaging Data from the Human Connectome Project *Brain Connect.* **6** 669–80 Online: http://online.liebertpub.com/doi/10.1089/brain.2016.0435

Carter A R, Astafiev S V., Lang C E, Connor L T, Rengachary J, Strube M J, Pope D L W, Shulman G L and Corbetta M 2010 Resting interhemispheric functional magnetic resonance imaging connectivity predicts performance after stroke *Ann. Neurol.* **67** 365–75

Chai X J, Castañán A N, Öngür D and Whitfield-Gabrieli S 2012 Anticorrelations in resting state networks without global signal regression *Neuroimage* **59** 1420–8

Chang C, Metzger C D, Glover G H, Duyn J H, Heinze H J and Walter M 2013 Association between heart rate variability and fluctuations in resting-state functional connectivity *Neuroimage* **68** 93–104 Online: http://dx.doi.org/10.1016/j.neuroimage.2012.11.038

Deboer R W, Karemaker J M and Strackee J 1984 Comparing spectra of a series of point events particularly for heart rate variability data *IEEE Trans. Biomed. Eng.* **BME-31** 384–7

Delpy D T, Cope M, van der Zee P, Arridge S, Wray S and Wyatt J 1988 Estimation of optical pathlength through tissue from direct time of flight measurement. *Phys. Med. Biol.* **33** 1433–42

Feinberg D A, Vu A T and Beckett A 2016 Pushing the limits of ultra-high resolution human brain imaging with SMS-EPI demonstrated for columnar level fMRI *Neuroimage* **164** 155–63

Fox M D, Zhang D, Snyder A Z and Raichle M E 2009 The global signal and observed anticorrelated resting state brain networks. *J. Neurophysiol.* **101** 3270–83 Online: http://www.ncbi.nlm.nih.gov/pubmed/19339462

Franklin K B J and Paxinos G 2008 *The Mouse Brain in Stereotaxic Coordinates* (Academic Press)

Fransson P and Marrelec G 2008 The precuneus/posterior cingulate cortex plays a pivotal role in the default mode network: Evidence from a partial correlation network analysis *Neuroimage* **42** 1178–84

Glasser M F, Coalson T S, Robinson E C, Hacker C D, Harwell J, Yacoub E, Ugurbil K, Andersson J, Beckmann C F, Jenkinson M, Smith S M and Van Essen D C 2016 A multi-modal parcellation of human cerebral cortex *Nature* **536** 171–8 Online: http://www.nature.com/doifinder/10.1038/nature18933

Gotts S J, Simmons W K, Milbury L A, Wallace G L, Cox R W and Martin A 2012 Fractionation of social brain circuits in autism spectrum disorders *Brain* **135** 2711–25

Greicius M D, Flores B H, Menon V, Glover G H, Solvason H B, Kenna H, Reiss A L and Schatzberg A F 2007 Resting-state functional connectivity in major depression: Abnormally increased contributions from subgenual cingulate cortex and thalamus *Biol. Psychiatry* **62** 429–37

Guevara E, Sadekova N, Girouard H and Lesage F 2013 Optical imaging of resting-state functional connectivity in a novel arterial stiffness model *Biomed. Opt. Express* **4** 2332–46 Online: http://www.pubmedcentral.nih.gov/articlerender.fcgi?artid=3829531&tool=pmcentrez&rendertype=abstract

Guttman L 1940 Multiple rectilinear prediction and the resolution into components * *Psychometrika* **5** 75–99

Haglund M M and Hochman D W 2007 Imaging of intrinsic optical signals in primate cortex during epileptiform activity *Epilepsia* **48** 65–74

Ishizuka T, Kakuda M, Araki R and Yawo H 2006 Kinetic evaluation of photosensitivity in genetically engineered neurons expressing green algae light-gated channels *Neurosci. Res.* **54** 85–94

Ivanov P C H, Liu K K L and Bartsch R P 2016 Focus on the emerging new fields of network physiology and network medicine *New J. Phys.* **18** Online: http://stacks.iop.org/1367-2630/18/i=10/a=100201

Kocsis L, Herman P and Eke A 2006 The modified Beer-Lambert law revisited *Phys. Med. Biol.* **51** N91-8

Lin A, Liu K K L, Bartsch R P and Ivanov P C 2016 Delay-correlation landscape reveals characteristic time delays of brain rhythms and heart interactions *Philos. Trans. R. Soc. London A Math. Phys. Eng. Sci.* **374** Online: http://rsta.royalsocietypublishing.org/content/374/2067/20150182

Liu T T, Nalci A and Falahpour M 2017 The global signal in fMRI: Nuisance or Information? *Neuroimage* **150** 213–29

Lynall M, Bassett D S, Kerwin R, Mckenna P J, Kitzbichler M, Müller U and Bullmore E 2010 Functional connectivity and brain networks in schizophrenia *J. Neurosci.* **30** 9477–87

Ma Y, Shaik M A, Kim S H, Kozberg M G, Thibodeaux D N, Zhao H T, Yu H and Hillman E M C 2016 Wide-field optical mapping of neural activity and brain haemodynamics: considerations and novel approaches *Philos. Trans. R. Soc. B Biol. Sci.* **371** 20150360 Online: http://rstb.royalsocietypublishing.org/lookup/doi/10.1098/rstb.2015.0360

Marrelec G, Krainik A, Duffau H, Pelegrini-Issac M, Lehericy S, Doyon J and Benali H 2006 Partial

correlation for functional brain interactivity investigation in functional MRI *Neuroimage* **32** 228–37

Mateo C, Knutsen P M, Tsai P S, Shih A Y and Kleinfeld D 2017 Entrainment of arteriole vasomotor fluctuations by neural activity is a basis of blood-oxygenation-level-dependent "Resting-state" connectivity *Neuron* **96** 936–48 Online: http://linkinghub.elsevier.com/retrieve/pii/S0896627317309807

Mayhew J, Johnston D, Berwick J, Jones M, Coffey P and Zheng Y 2000 Spectroscopic analysis of neural activity in brain: Increased oxygen consumption following activation of barrel cortex *Neuroimage* **12** 664–75 Online: http://linkinghub.elsevier.com/retrieve/pii/S1053811900906566

Mitsuyuki N, Masashi N, Yoshinari M and Yamamoto M 1997 Spectral distortion properties of the integral pulse frequency modulation model **44** 419–26

Murphy K, Birn R M, Handwerker D A, Jones T B and Bandettini P A 2009 The impact of global signal regression on resting state correlations: Are anti-correlated networks introduced? *Neuroimage* **44** 893–905 Online: http://dx.doi.org/10.1016/j.neuroimage.2008.09.036

Murphy K, Birn R M and Bandettini P A 2013 Resting-state fMRI confounds and cleanup *Neuroimage* **80** 349–59

Öngür D, Lundy M, Greenhouse I, Shinn A K, Menon V, Cohen B M and Renshaw P F 2010 Default mode network abnormalities in bipolar disorder and schizophrenia *Psychiatry Res. - Neuroimaging* **183** 59–68 Online: http://dx.doi.org/10.1016/j.pscychresns.2010.04.008

Pomeranz B, Macaulay R J B, Caudill M A, Kutz I, Adam D, Gordon D, Kilborn K M, Barger A C, Shanon D C, Cohen R J and Benson H 1985 Assessment of autonomic function by heart rate spectral analysis in humans *Am. J. Physiol.* **248** H151–3

Pouratian N, Sicotte N, Rex D, Martin N A, Becker D, Cannestra A F and Toga A W 2002 Spatial/temporal correlation of BOLD and optical intrinsic signals in humans Magn. Reson. Med. 47 766–76

Power J D, Plitt M, Laumann T O and Martin A 2017 Sources and implications of whole-brain fMRI signals in humans *Neuroimage* **146** 609–25 Online: http://dx.doi.org/10.1016/j.neuroimage.2016.09.038

Sforazzini F, Schwarz A J, Galbusera A, Bifone A and Gozzi A 2014 Distributed BOLD and CBV-weighted resting-state networks in the mouse brain *Neuroimage* **87** 403–15 Online: http://linkinghub.elsevier.com/retrieve/pii/S1053811913009865

Sheline Y I, Price J L, Yan Z and Mintun M A 2010 Resting-state functional MRI in depression unmasks increased connectivity between networks via the dorsal nexus *Proc. Natl. Acad. Sci.* **107** 11020–5 Online: http://www.pubmedcentral.nih.gov/articlerender.fcgi?artid=2890754&tool=pmcentrez&rendertype=abstract

Sheth S A, Nemoto M, Guiou M, Walker M, Pouratian N and Toga A W 2004 Linear and nonlinear relationships between neuronal activity, oxygen metabolism, and hemodynamic responses *Neuron* **42** 347–55

Shmueli K, van Gelderen P, de Zwart J A, Horovitz S G, Fukunaga M, Jansma J M and Duyn J H 2007 Low-frequency fluctuations in the cardiac rate as a source of variance in the resting-state fMRI BOLD signal *Neuroimage* **38** 306–20

Sigurdsson T, Stark K L, Karayiorgou M, Gogos J A and Gordon J A 2010 Impaired hippocampal-prefrontal synchrony in a genetic mouse model of schizophrenia *Nature* **464** 763–7 Online: http://dx.doi.org/10.1038/nature08855

Tohmi M, Takahashi K, Kubota Y, Hishida R and Shibuki K 2009 Transcranial flavoprotein fluorescence imaging of mouse cortical activity and plasticity *J. Neurochem.* **109** 3–9

Veasey S C, Valladares O, Fenik P, Kapfhamer D, Sanford L, Benington J and Bucan M 2000 An automated system for recording and analysis of sleep in mice. *Sleep* **23** 1025–40

van den Heuvel M P and Hilleke E H P 2010 Exploring the brain network: A review on resting-state fMRI functional connectivity *Eur. Neuropsychopharmacol.* **20** 519–34 Online: http://dx.doi.org/10.1016/j.euroneuro.2010.03.008%5Cnpapers3://publication/doi/10.1016/j.euroneuro.2010.03.008

Wang Y, Kang J, Kemmer P B and Guo Y 2016 An efficient and reliable statistical method for estimating functional connectivity in large scale brain networks using partial correlation *Front. Neurosci.* **10** 1–17

White B R, Bauer A Q, Snyder A Z, Schlaggar B L, Lee J M and Culver J P 2011 Imaging of functional connectivity in the mouse brain *PLoS One* **6** e16322

Yoshida Y, Nakagawa D, Karashima A, Nakao M and Katayama N 2015a Performance Evaluation of Light Source Noise Reduction Algorithm Based on Independent Component Analysis for Optical Intrinsic Signal Data *Trans. Japanese Soc. Med. Biol. Eng.* **53** 328–35

Yoshida Y, Nakagawa D, Karashima A, Nakao M and Katayama N 2015b Reduction of light source noise from optical intrinsic signals of mouse neocortex by using independent component analysis *Conf. Proc. IEEE Eng Med. Biol. Soc.* vol 2015–Novem pp 6277–80

Zhou Y, Liang M, Tian L, Wang K, Hao Y, Liu H, Liu Z and Jiang T 2007 Functional disintegration in paranoid schizophrenia using resting-state fMRI *Schizophr. Res.* **97** 194–205 Online: http://linkinghub.elsevier.com/retrieve/pii/S0920996407002393